

Kinematic and Dynamic Analysis of the 2-DOF Spherical Wrist of Orthoglide 5-axis

Raza UR-REHMAN, Stephane CARO, Damien CHABLAT and Philippe WENGER

Institut de Recherche en Communication et Cybernétique de Nantes, UMR CNRS 6597, 1 rue de la Noë, 44321, Nantes Cedex 03, France

Raza.Ur-Rehman@ircryn.ec-nantes.fr

Stephane.Caro@ircryn.ec-nantes.fr

Damien.Chablat@ircryn.ec-nantes.fr

Philippe.Wenger@ircryn.ec-nantes.fr

Abstract - This paper deals with the kinematics and dynamics of a two degree of freedom spherical manipulator, the wrist of Orthoglide 5-axis. The latter is a parallel kinematics machine composed of two manipulators: i) the Orthoglide 3-axis; a three-dof translational parallel manipulator that belongs to the family of Delta robots, and ii) the Agile eye; a two-dof parallel spherical wrist. The geometric and inertial parameters used in the model are determined by means of a CAD software. The performance of the spherical wrist is emphasized by means of several test trajectories. The effects of machining and/or cutting forces and the length of the cutting tool on the dynamic performance of the wrist are also analyzed. Finally, a preliminary selection of the motors is proposed from the velocities and torques required by the actuators to carry out the test trajectories.

KEYWORDS: Spherical mechanism/Agile eye/Orthoglide 5-axis/kinematics/dynamics

Résumé - L'objet de ce papier est de présenter une étude cinématique et dynamique d'un mécanisme sphérique à deux degrés de liberté (ddls), le poignet de l'Orthoglide 5 axes. Ce dernier est une machine à cinématique parallèle composée de deux manipulateurs: i) l'Orthoglide 3 axes, manipulateur parallèle à trois ddls de translation qui appartient à la famille des robots de type Delta, et ii) l'Oeil Agile; poignet sphérique à deux ddls. Les paramètres géométriques et inertiels sont déterminés à l'aide d'un logiciel de CAO. La performance du poignet sphérique est soulignée par plusieurs trajectoires tests. Les effets de l'effort d'usinage et de la longueur de l'outil sur la performance dynamique du poignet sont également analysés. Enfin, une sélection préliminaire des moteurs est proposée à partir des vitesses et des couples requis par les actionneurs afin d'effectuer les trajectoires désirées

MOTS-CLÉS: Mécanisme sphérique/Oeil Agile /Orthoglide 5-axis/cinématique/dynamique

1 Introduction

A spherical mechanism can orient or move the end-effector about the center of rotation of the mechanism. A typical 3-DOF spherical manipulator or wrist provides the three dimensional (3D) rotations like a human hand but in most robotics applications only 2D rotations are sufficient. Rotation about the axis of symmetry of the end-effector is not necessary and if required, can be provided independently.

Several researchers have worked in the domain of spherical mechanisms mainly for the applications of end-effector orientations. One of the earlier spherical mechanisms is that presented in the work of Asada and Cro Granito [1], which is a three-degree-of-freedom (dof) spherical wrist with coaxial motors and three kinematics chains. In 1989, W. M. Craver [2], analysed a spherical robotic shoulder module. Other major publications to the research and development of the spherical mechanism are the work of Gosselin et al [3, 4, 5] where optimum kinematic designs of different types of spherical parallel mechanisms are presented. The Agile Eye, one of the most famous spherical mechanisms designed by Gosselin and Hamel [6], is a 3-dof parallel mechanism developed to control the orientation of a camera. Several mechanisms have been designed for diverse applications from the Agile Eye. Spherical mechanisms can be implemented in radar applications [7], camera manipulations [8] and surgical applications [9]. Cavallo and Michelini [10] introduced a 3-dof spherical parallel mechanism composed of three identical kinematic chains to orient the propeller and duct of a small autonomous underwater vehicle (AUV). Main contributions for the design and analysis of spherical mechanisms are reported in [1, 3, 4, 5, 6, 11, 12, 13, 14, 15, 16].

This paper focuses on the kinematic and dynamic analysis of the two dof spherical wrist of Orthoglide 5-axis, a five dof parallel kinematics machine developed for high speed operations. Here, we focus on the evaluation of the velocities, accelerations and the torques required by the actuators of the spherical wrist. First, the kinematics of the spherical wrist is studied and then its dynamics is analyzed by means of the Newton-Euler approach. The geometric and inertial parameters are determined with a CAD software. The performance of the manipulator is emphasized by means of several test trajectories. Finally, the actuators are selected in the catalogue based on the velocities and torques required by the actuators to carry out the test trajectories.

2 Orthoglide 5-axis

Orthoglide 5-axis, illustrated in Figure 1, is derived from a 3-dof translating manipulator, the Orthoglide 3-axis and a 2-dof spherical wrist [17].

Orthoglide 3-axis, is a Delta-type PKM [18] dedicated to 3-axis rapid machining applications developed at the Institut de Recherche en Communications et Cybernétique de Nantes (IRCCyN) [19]. This mechanism is composed of three identical legs. Each leg is made up of a prismatic joint, a revolute joint, a parallelogram joint and another revolute joint. Only the prismatic joints of each leg are actuated.

It gathers the advantages of both serial and parallel kinematic architectures such as regular workspace, homogeneous performances, good dynamic performances and stiffness. The interesting features of Orthoglide 3-axis are a regular dexterous workspace, uniform kinetostatic performances in all directions, good compactness [20] and high stiffness [21].

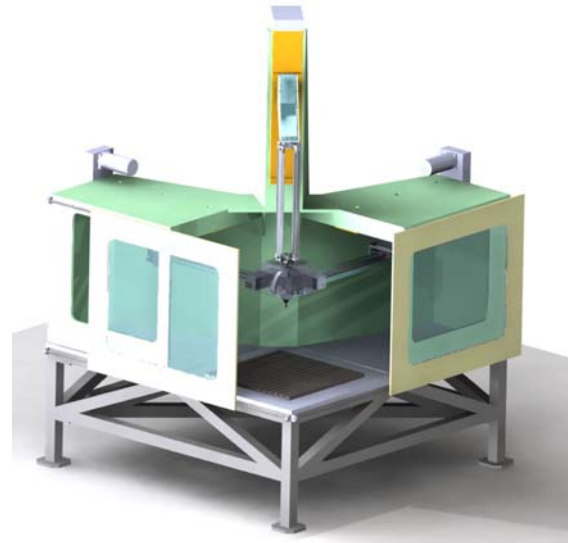


Figure 1. Orthoglide 5-axis

The two-dof spherical wrist that is implemented in Orthoglide 5-axis is derived from the Agile Eye, a three-dof spherical wrist [6]. Here, the two-dof spherical wrist is designed to obtain high stiffness [22]. A CAD model of the latter is shown in Figure 2.

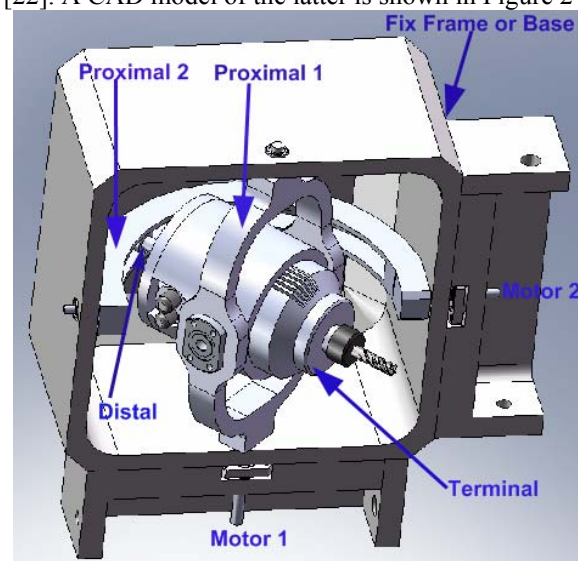


Figure 2. Spherical wrist of Orthoglide 5-axis

3 Spherical wrist kinematic model

Reference frames and DH parameters

The spherical wrist of Orthoglide 5-axis is composed of a closed kinematic chain made up of five components: proximal-1, proximal-2, distal, terminal and the base. These five links are connected by means of revolute joints, of which axes intersect at the center of the mechanism. Besides, only the two revolute joints connected to the base of the wrist are actuated. The distal has an imaginary axis of rotation passing through the intersection point of other joint axis and perpendicular to the plane of proximal-2. A unit vector \mathbf{e}_i and a reference frame R_i are associated to each joint with Z_i -axis and \mathbf{e}_i being coincident. The angle between \mathbf{e}_1 and \mathbf{e}_2 is denoted by α_0 and the angle between \mathbf{e}_i and \mathbf{e}_{i+2} is denoted by α_i , for $i=1 \dots 4$.

Reference frame R_1 is defined in such a way that Z_1 -axis coincides with \mathbf{e}_1 and \mathbf{e}_2 lies in the X_1Z_1 -plane. Similarly R_2 has its Z_2 -axis in the direction of \mathbf{e}_2 and \mathbf{e}_1 lies in the X_2Z_2 -plane. Reference frame R_i ($i=3, 4, 5, 6$) with $Z_i = \mathbf{e}_i$ are defined by the rotation of frame R_{i-2} and following the Denavit-Hartenberg conventions. DH-conventions for Orthoglide wrist mechanism are summarized as follow:

- Z_i : axis of the i^{th} joint;
- X_i : common perpendicular to Z_{i-2} and Z_i ;
- Y_i : respecting the right hand rule;
- a_i : distance between Z_i and Z_{i+2} ;
- b_i : distance between X_i and X_{i+2} ;
- α_i : angle between Z_i and Z_{i+2} about X_{i+2} ;
- θ_i : angle between X_i and X_{i+2} about Z_i .

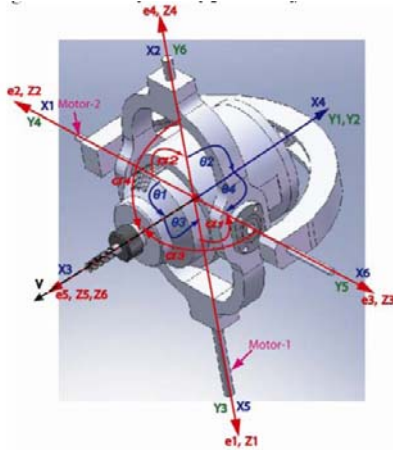


Figure 3. Orientations of reference frames according to DH-Conventions for Orthoglide Wrist

As all joints axes intersect at a common point, the origin of all the frames are the same i.e., $a_i=b_i=0$. Figure 3 shows the orientations of reference frames attached to the Orthoglide wrist according to the DH convention, α_i being equal to $\pi/2$. In the home configuration, $\theta_1=\theta_4=-\pi/2$ and $\theta_2=\theta_3=+\pi/2$.

Kinematics of Orthoglide wrist

The kinematics of the wrist of Orthoglide 5-axis is similar to the one of the Agile Eye introduced in [8].

However, the architecture is not the same as the distal and the proximal – 2 are different. Nevertheless, we can easily derive the kinematic and dynamic models of the wrist of Orthoglide 5-axis from [8]. Moreover, the influence of the external and/or machining forces on the dynamic performance is also considered.

Kinematic equations of the Orthoglide wrist are developed with the help of the reference frames defined above and the DH-parameters. It is noteworthy that the camera manipulator [8] and the Orthoglide wrist are analogous. However, subsequent modifications are made. Vector \mathbf{v} depicts the orientation of the wrist end-effector (cutting tool etc), which is defined in reference frame R_5 by three angles β_1, β_2 & γ illustrated in Figure 4:

- β_1 being the angle between \mathbf{e}_5 and the projection of \mathbf{v} to \mathbf{e}_3 - \mathbf{e}_5 plane;
- β_2 being the angle between \mathbf{v} and \mathbf{e}_3 - \mathbf{e}_5 plane;
- γ being the angle between \mathbf{v} and \mathbf{e}_3 .

The expression of \mathbf{v} in R_5 is then defined as,

$$[\mathbf{v}]_5 = [\sin \beta_2 \quad \sin \beta_1 \cos \beta_2 \quad \cos \beta_1 \cos \beta_2]^T$$

Since vectors \mathbf{v} and \mathbf{e}_5 coincide (Figure 3), i.e. $\mathbf{v} = \mathbf{e}_5$ hence $\beta_1 = \beta_2 = 0$ and $\gamma = \pi/2$.

The orientation of vector \mathbf{v} is defined in reference frame R_1 by the pan (φ_1) and tilt (φ_2) angles as shown in Figure 4. With the definitions of φ_1 and φ_2 , the components of \mathbf{v} in R_1 are given by:

$$[\mathbf{v}]_1 = [\cos \varphi_1 \cos \varphi_2 \quad \sin \varphi_1 \cos \varphi_2 \quad \sin \varphi_2]^T$$

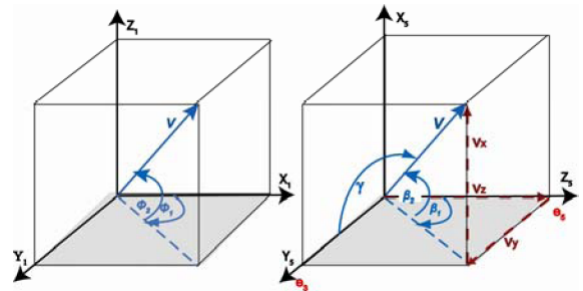


Figure 4. Definition of \mathbf{v} in R_1 and R_5

Finally, the inverse kinematic problem of the wrist can be derived from \mathbf{v} , α , β_1 , β_2 , γ , φ_1 and φ_2 . The relations for the joints variables ($\theta_1, \theta_2, \theta_3, \theta_4$) are summarized below [8] (in these relations, c and s stands for *cosine* and *sine* functions respectively).

$$\theta_1 = \tan^{-1} \left[\frac{2T}{1-T^2} \right]$$

where

$$T = \frac{-B + \sqrt{B^2 - 4AC}}{2A} \begin{cases} A = v_z c \alpha_1 + v_y s \alpha_1 - c \gamma \\ B = 2v_x s \alpha_1 \\ C = v_z c \alpha_1 - v_y c \alpha_1 - c \gamma \end{cases}$$

$$\theta_3 = \tan^{-1} \left(\frac{a \times e + b \times d}{a \times d - b \times e} \right)$$

where

$$\begin{aligned} a &= s \beta_2 & b &= s \alpha_3 c \beta_1 c \beta_2 - c \alpha_3 s \beta_1 c \beta_2 \\ d &= v_x c \theta_1 + v_y s \theta_1 & e &= -v_x s \theta_1 c \alpha_1 + v_y c \theta_1 c \alpha_1 + v_z c \alpha_1 \end{aligned}$$

$$\theta_2 = \tan^{-1} \left(2T / (1 - T_2^2) \right)$$

where

$$u_x = s\theta_1 s\alpha_1 c\alpha_3 + s\theta_1 c\theta_3 c\alpha_1 s\alpha_3 + c\theta_1 s\theta_3 s\alpha_3$$

$$u_y = -c\theta_1 s\alpha_1 c\alpha_3 - c\theta_1 c\theta_3 c\alpha_1 s\alpha_3 + s\theta_1 s\theta_3 s\alpha_3$$

$$u_z = c\alpha_1 c\alpha_3 - c\theta_3 c\alpha_1 c\alpha_3$$

$$A_2 = u_x s\alpha_0 c\alpha_2 + u_y s\alpha_2 + u_z c\alpha_0 c\alpha_2 - c\alpha_4$$

$$B_2 = 2(u_x c\alpha_0 s\alpha_2 - u_z s\alpha_0 s\alpha_2)$$

$$C_2 = u_x s\alpha_0 c\alpha_2 - u_y s\alpha_2 + u_z c\alpha_0 c\alpha_2 - c\alpha_4$$

$$T_2 = \left(-B_2 - \sqrt{B_2^2 - 4A_2 C_2} \right) / 2A_2$$

$$\theta_4 = \tan^{-1} (s_4 / c_4)$$

where

$$a_4 = -u_x (s\alpha_0 s\alpha_2 - s\theta_2 c\alpha_0 c\alpha_2) \quad , b_4 = -u_y c\theta_2 c\alpha_2$$

$$d_4 = -u_z (c\alpha_0 c\alpha_2 + s\theta_2 s\alpha_0 c\alpha_2)$$

$$s_4 = \frac{u_x c\theta_2 c\alpha_0 + u_y s\theta_2 - u_z c\theta_2 s\alpha_0}{s\alpha_4} \quad , c_4 = \frac{a_4 + b_4 + d_4}{s\alpha_4}$$

Similarly, analytical relations of joints rates, i.e. joints velocities and acceleration can be obtained with the help of the previous relations of joint displacements and unit vectors e_i . Otherwise, numerical techniques, like finite difference method can be used to obtain joint velocities and accelerations.

4 Wrist dynamics

Dynamic analysis is of primary importance to investigate the forces and moments applied to the actuators to carry out a desired task or motion by the manipulator. Dynamic analysis of 2-DOF camera manipulator is presented in [8] where Newton-Euler approach is used. A similar methodology is also used here for Orthoglide wrist.

As a first step, wrist joints displacements are calculated from the kinematic model as discussed in the previous section. Velocities and accelerations of each component are obtained with the help of kinematic modeling, which has not been presented here because of space limitations. Also first and second derivatives of the unit vectors e_1, e_2, e_3, e_4 and e_5 are calculated. For the detailed relations of these calculations reader is referred to [8]. Finally a system of equilibrium equations, obtained from the free body diagrams of each wrist component, is used to get the relations of actuators torques. A flow chart of the torques calculations is given in Figure 5

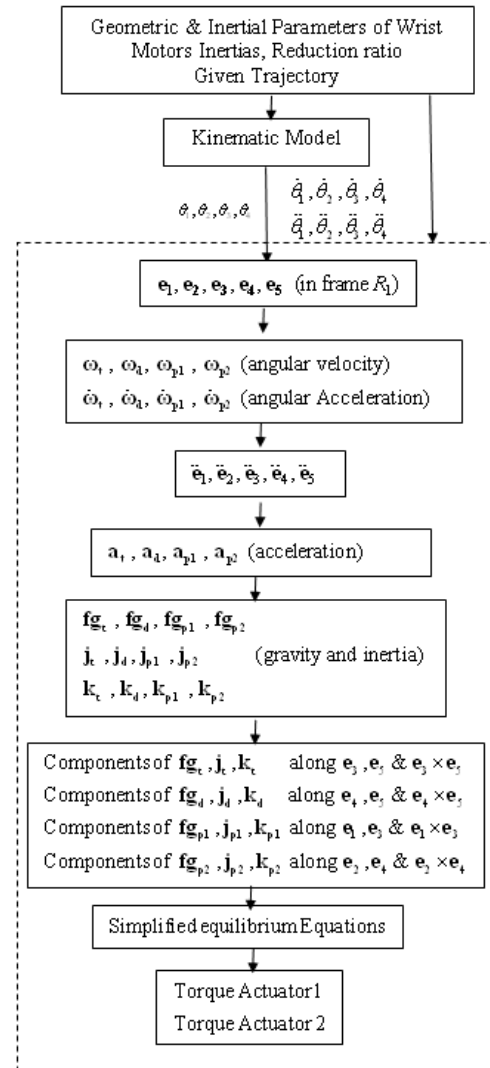


Figure 5. Flow chart of the dynamic model

Equilibrium equations

In this section, the methodology to obtain equilibrium equations of the Orthoglide wrist is presented. The following assumptions are made:

- friction forces are neglected;
- a spherical joint is assumed between the distal and the terminal link to have isostatic mechanism;
- a planar joint between the distal and the proximal-2.

With these assumptions, the free-body diagrams (FBD) of terminal, distal, proximal-1 and proximal-2 are drawn, as shown in Figure 6 to 9. Forces and moments acting on four moving wrist components are summarized below:

- two forces **A** and **B** and one moment **M** are exerted to the terminal;
- two force **C** and **D** are exerted to the distal;
- two forces **G** and **H** and two moments **N** and **P** are exerted to the proximal-1;
- two forces **E** and **F** and a moment **R** are exerted to the proximal-2.

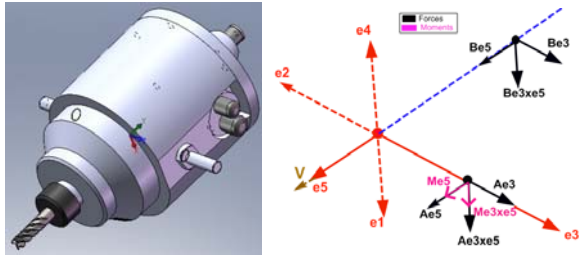


Figure 6. CAD model and FBD of terminal

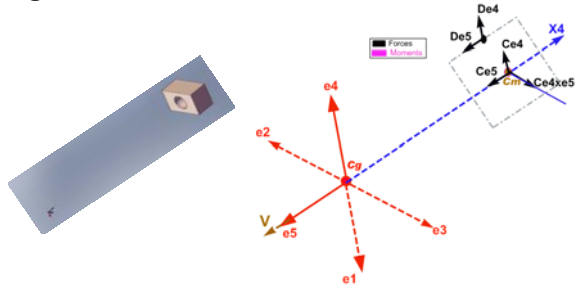


Figure 7. CAD model and FBD of distal

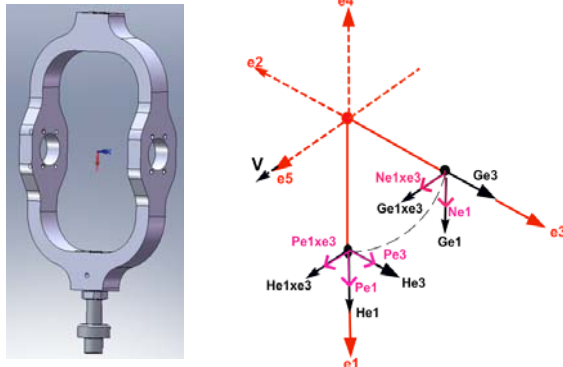


Figure 8. CAD model and FBD of proximal-1

These forces and moments are resolved into orthogonal components with respect to the attached unit vectors. Equilibrium equations are written for each moving component (resulting 24 equations). For instance, set of equilibrium equations for the terminal (Figure 6) is given by:

$$\begin{aligned} \sum F_{e3} &= A_{e3} + B_{e3} + F_{gte3} = J_{te3} \\ \sum F_{e5} &= A_{e5} + B_{e5} + F_{gte5} = J_{te5} \\ \sum F_{e3xe5} &= A_{e3xe5} + B_{e3xe5} + F_{gte3xe5} = J_{te3xe5} \\ \sum M_{e3} &= -L_{te5}B_{e3xe5} - l_{te3xe5}F_{gte5} + l_{te5}F_{gte3xe5} = K_{te3} \\ \sum M_{e5} &= M_{e5} - L_{te3}A_{e3xe5} - l_{te3}F_{gte3xe5} + l_{te3xe5}F_{gte5} = K_{te5} \\ \sum M_{e3xe5} &= M_{e3xe5} + L_{te5}B_{e3} + L_{te3}A_{e5} + l_{te3}F_{gte5} - l_{te5}F_{gte3} = K_{te3xe5} \end{aligned}$$

Where F_{gte3} , F_{gte5} , $F_{gte3xe5}$ are the gravity terms, K_{gte3} , K_{gte5} , $K_{gte3xe5}$ are the inertial terms (function of angular velocity, acceleration and inertia matrix) and J_{gte3} , J_{gte5} , $J_{gte3xe5}$ are the inertial forces (function of linear acceleration and mass) of the terminal along e_3 , e_5 and e_3xe_5 directions respectively. Other variables used in these equations are defined in the next section.

Along with equilibrium equations, compatibility equations i.e., action-reaction equilibrium equations at terminal-distal, terminal-proximal-1 and distal-proximal-2 interaction points are also written

(resulting 10 equations). The system of equations so obtained can be solved to obtain the torques experienced by the wrist actuators i.e. P_{e1} and R_{e2} .

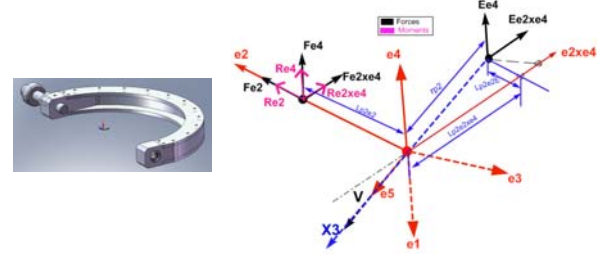


Figure 9. CAD model and FBD of proximal-2

Wrist dynamic parameters

The input parameters of the dynamic model of the Orthoglide wrist are:

- mass of each component (m_b, m_d, m_{p1}, m_{p2});
- distance between wrist geometric centre and centre of mass of each component (l);
- distance between wrist geometric centre and the point of application of force (L);
- inertia matrices of wrist component (I_b, I_d, I_{p1}, I_{p2});
- inertia of actuators (K_{m1}, K_{m2});
- reduction ratios of actuators (η_{m1}, η_{m2}).

The mass and inertial parameters are determined by means of a CAD software. The geometric parameters (l or L) are determined from the drawings or CAD models of wrist components along with corresponding unit vectors.

Effect of machining force on actuators torques

So far we have not taken into account the effect of the machining or cutting forces on the wrist dynamics. To cater for these forces we redraw the free body diagram of the terminal, with three components of cutting force $f_c = [F_{ce3} \quad F_{ce5} \quad F_{ce3xe5}]$

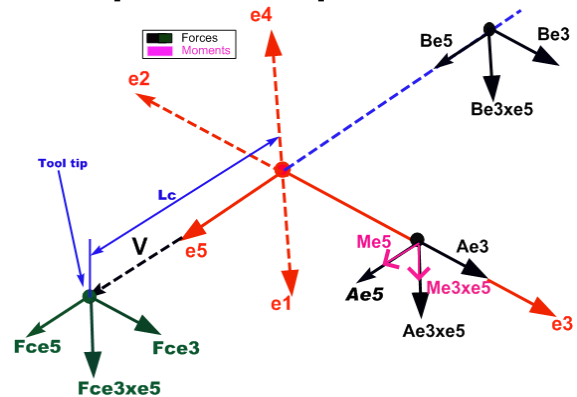


Figure 10. Terminal FBD with machining forces

The distance between the tool tip and geometric center of wrist is taken as L_c (Figure 10). For this free body diagram, equilibrium equations are rewritten and new set of actuators equations are obtained.

Motors parameters

In the preliminary design stage, FFA 20-80 harmonic drive motors are selected for both actuators. Motors specifications taken from the motor catalogue are given in Table 1 and their inertia is incorporated in the dynamic equations.

Table 1. Motors parameters

FFA 20-80 Harmonic Drive	
Nominal speed	2500 rpm
Maximum speed	6500 rpm
Maximum torque at output shaft	74 Nm
Continuous torque	23 Nm
Motor moment of inertia	0.00262 kg.m ⁴
Motor power	800 W

Trajectories generations

Two test trajectories are introduced for the Orthoglide 5-axis. Corresponding to these trajectories, inverse kinematic problem for the wrist is solved. The trajectories are defined as follows:

- Traj. I: semi-circular trajectory in vertical or YZ-plane defined by radius R and trajectory angles ψ and δ (Figure 11)

$$\mathbf{v} = \begin{bmatrix} v_x \\ v_y \\ v_z \end{bmatrix} = \begin{bmatrix} 0 \\ -\sin \delta \\ -\cos \delta \end{bmatrix} \text{ where } \delta \text{ varies from } \pi/6 \text{ to } 5\pi/6 \text{ while } \psi \text{ varies from } 0 \text{ to } \pi.$$

- Traj. II: circular trajectory in horizontal or XY-plane defined by radius R, constant orientation angle γ of vector \mathbf{v} with Z-axis and angle δ (Figure 12)

$$\mathbf{v} = \begin{bmatrix} v_x \\ v_y \\ v_z \end{bmatrix} = \begin{bmatrix} \sin \gamma \cos \delta \\ \sin \gamma \sin \delta \\ -\cos \gamma \end{bmatrix}$$

where δ varies from 0 to 2π

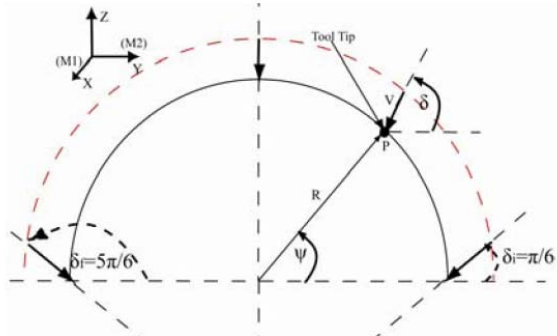


Figure 11.Orientation of vector \mathbf{v} (Traj I)

5 Kinematic and dynamic analyses

The kinematics of the Orthoglide wrist is analysed for the two test trajectories. The velocity of the end-effector, located on point P (on the tip of the wrist tool), throughout the trajectory, is taken as constant

i.e. $V_p = 1$ m/s and accordingly trajectory time is calculated with constant velocity.

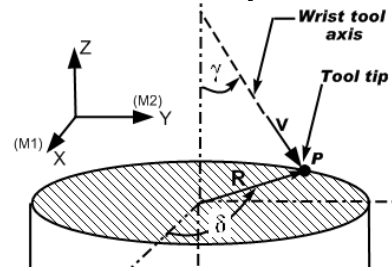


Figure 12. Orientation of vector \mathbf{v} (Traj II)

Figure 13 shows the plots of position, velocity and acceleration of the joints for Traj. II with $R = 0.25$ m and $\gamma = 45^\circ$. For the same trajectory, dynamic model is used to calculate the actuators torques, as shown in Figure 14.

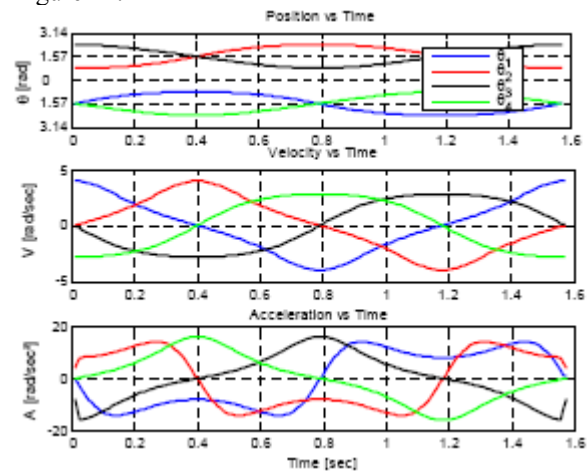


Figure 13. Position, velocity and acceleration of articulations (Traj II)

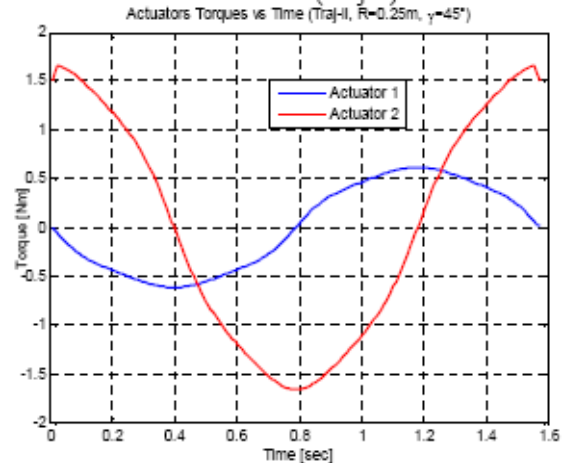


Figure 14. Actuators torques vs time (Traj. II)

Table 2 shows the maximum values of the kinematic and dynamic parameters for Traj. II for $R = 0.05, 0.1, 0.15$ and 0.25 m and for $\gamma = 30^\circ, 45^\circ$ and 60° where T_1 and P_1 (resp. T_2 and P_2) is the torque and the power of actuators 1 (resp. 2). Results show that the trajectory with $R = 0.5$ m and $\gamma = 60^\circ$ is more critical as compared to the other trajectories; it requires higher maximum velocities, accelerations and torques. Maximum values of actuators torques are also shown in Figure 15.

Table 2. Kinematics and dynamics peak values with no external forces (Traj II)

γ [deg]	Radius [m]	Max Velocity [rad/s]				Max Acceleration [rad/s ²]				Max Torque [Nm]		Max Power [W]	
		$\dot{\theta}_1$	$\dot{\theta}_2$	$\dot{\theta}_3$	$\dot{\theta}_4$	$\ddot{\theta}_1$	$\ddot{\theta}_2$	$\ddot{\theta}_3$	$\ddot{\theta}_4$	T_1	T_2	P_1	P_2
30	0.250	2.31	2.31	2.00	2.00	7.29	7.29	9.21	9.21	0.68	1.22	0.64	1.20
	0.150	3.84	3.84	3.33	3.33	20.24	20.24	25.59	25.59	0.90	1.67	1.58	2.77
	0.100	5.77	5.77	5.00	5.00	45.54	45.54	57.58	57.59	1.35	2.55	3.89	6.43
	0.050	11.53	11.53	10.00	10.00	182.15	182.15	230.30	230.35	3.75	7.29	24.33	37.46
45	0.250	3.99	3.99	2.83	2.83	13.96	13.96	15.92	15.92	0.94	1.73	1.26	2.43
	0.150	6.65	6.65	4.71	4.71	38.78	38.78	44.22	44.22	1.23	2.37	3.86	5.97
	0.100	9.98	9.98	7.07	7.07	87.26	87.26	99.48	99.48	1.79	3.62	11.14	14.69
	0.050	19.96	19.96	14.14	14.14	349.03	349.03	397.94	397.94	5.58	10.38	80.14	92.25
60	0.250	6.90	6.90	3.46	3.46	34.05	34.05	27.36	27.36	1.11	2.16	3.17	5.22
	0.150	11.49	11.49	5.77	5.77	94.59	94.59	75.99	75.99	1.54	3.03	13.47	15.78
	0.100	17.24	17.24	8.66	8.66	212.82	212.82	170.98	170.98	3.31	4.72	44.17	45.04
	0.050	34.48	34.48	17.32	17.32	851.30	851.30	683.92	683.92	12.94	13.84	347.23	320.89

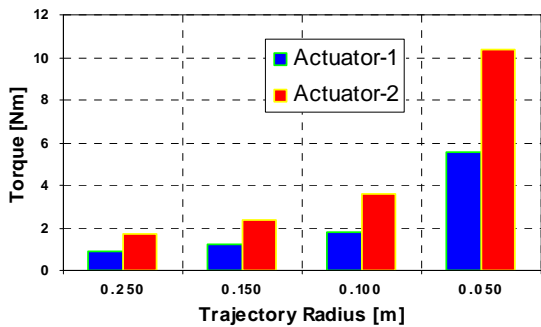


Figure 15. Actuators maximum torques vs trajectory radii ($\gamma=45^\circ$, Traj. II)

In order to analyse the effects of machining or cutting forces (see Figure 10), three equal components of \mathbf{f}_c are assumed, i.e.,

$$F_{ce3} = F_{ce3 \times e5} = F_{ce5} = F_c = \text{constant}$$

Actuators torques are calculated while considering the machining forces of different magnitudes and for trajectory radius of 0.15 m with $\gamma=45^\circ$. Three values of machining forces moment arm L_c are taken, i.e. $L_c=0.06, 0.11$ and 0.15 m. Results are shown in Figure 16 to 18.

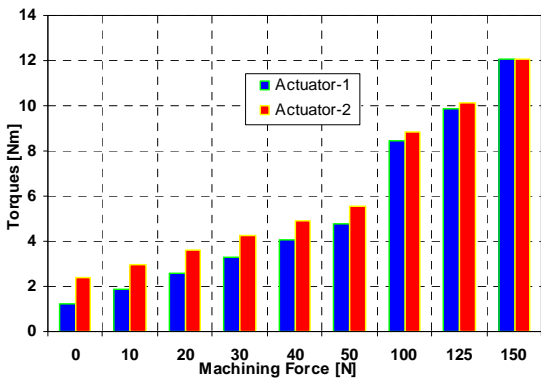


Figure 16. Actuators maximum torques with F_c ($L_c=0.06$ m, Traj. II)

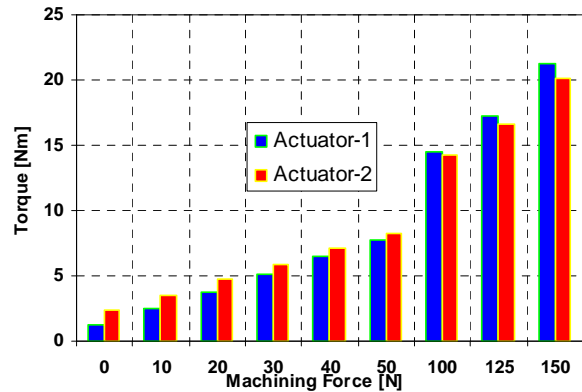


Figure 17. Actuators maximum torques with F_c ($L_c=0.11$ m, Traj. II)

Figure 18 shows that for the machining forces of 125 N and 150 N, actuators torques exceed the motors continuous torque (23 Nm) but still these are well below to the maximum motors torque (74 Nm). Hence for the given test trajectories considered motors can work for a range of machining forces. These results also represent the considerable influence of the length of the moment arm L_c of the machining forces (or the tool length) on the actuators torques.

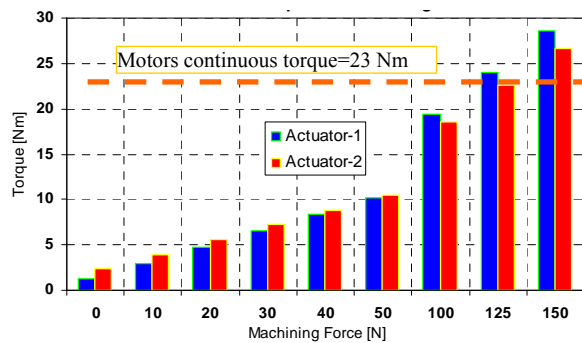


Figure 18. Actuators maximum torques with F_c ($L_c=0.15$ m, Traj. II)

6 Conclusions

This paper deals with the kinematics and dynamics of the spherical wrist of Orthoglide 5-axis. The kinematic and dynamic performances of the wrist were analyzed and its actuators primarily selection was proposed by means of several test trajectories. A methodology was introduced to evaluate the velocities, accelerations and torques required by the actuators. The influence of the machining forces as well as the tool length on the wrist actuators torques and powers was also studied. It turns out that the primarily selected motors with a continuous torque of 23 Nm and of power equal to 0.8 kW are suitable for the prototype of Orthoglide 5-axis. Finally, the following points will be taken into account in future works: (i) the friction between links has to be considered, (ii) planar joint between distal and proximal-2 should be analysed more precisely, (iii) weight of the machining tool should also be taken into consideration, and (iv) a larger range of trajectories should be analysed.

7 References

- [1] H. Asada, and C. Granito, "Kinematic and static characterization of wrist joints and their optimal design," Proc. IEEE Conf. Robotics and Automation, St. Louis, USA, March 25-28, 1985, pp. 244-250
- [2] W. M. Craver, "Structural analysis and design of a three-degree-of-freedom robotic shoulder module," M.S. thesis, The University of Texas at Austin, Department of Mechanical Engineering, 1989
- [3] C. Gosselin and J. Angeles, "The optimum kinematic design of a planar three degree of-freedom parallel manipulator," ASME Journal of Mechanisms, Transmission, and Automation in Design, vol. 110, pp. 35-41, 1988
- [4] C. Gosselin, and J. Angeles, "The optimum kinematic design of a spherical three-degree-of-freedom parallel manipulator," J. Mechanisms, Transmissions and Automation in Design, Vol. 111(2), 1989, pp.202-207
- [5] C. Gosselin, and E. Lavoie, "On the Kinematic Design of spherical three-dof parallel manipulators," The international Journal of Robotic Research. Vol. 12(4), 1993, pp. 394-402
- [6] C. Gosselin, and J.F. Hamel, "The agile eye: a high performance three-dof camera-orienting device," IEEE Int. conference on Robotics and Automation, San Diego, 1994, pp. 781-787
- [7] G.R. Dunlop and T.P. Jones, "Position analysis of a two DOF parallel mechanism- the Canterbury tracker," Mechanism and Machine Theory, Vol. 34(4), 1999, pp. 599-614
- [8] F. Caron, "Analyse et conception d'un manipulateur parallèle sphérique à deux degrés de liberté pour l'orientation d'une caméra," M.S. thesis, Laval University, Quebec, Canada, 1997
- [9] M.J.H. Lum, J. Rosen, M. N. Sinanan, B. Hannaford, 'Kinematic Optimization of Serial and Parallel Spherical Mechanism for a Minimally Invasive Surgical Robot,' IEEE Transactions on Biomedical Engineering, vol. 53(7), July 2006
- [10] E. Cavallo and R. Micheli, "A robotic equipment for the guidance of a vectored thruster auv," in Proc. 35th Int. Symp. Robotics ISR2004, vol. 1, Mars 2004, pp. 1- 6
- [11] C. Innocenti, and V. Parenti-Castelli, "Echelon form solution of direct kinematics for the general fully-parallel spherical wrist," Mechanism and Machine Theory, Vol. 28, No. 4, 1993, pp. 553 - 561
- [12] R.I. Alizade, N. R. Tagiyev, and J. Duffy, "A forward and reverse displacement analysis of an in-parallel spherical manipulator," Mechanism and Machine Theory, Vol. 29(1), 1994, pp.125-137
- [13] M. Karouia, and J. M. Hervè, "A three-dof tripod for generating spherical rotation," Advances in Robot Kinematics, Kluwer, 2000, pp.395-402
- [14] M. Karouia, and J. M. Hervè, "A Family of Novel Orientational 3-DOF Parallel Robots," Proc. RoManSy 14, Udine, Italy, July 1-4, 2002
- [15] L. W. Tsai, Robot analysis: The Mechanics of Serial and Parallel Manipulators, John Wiley & Sons, New York, 1999
- [16] J.-P. Merlet, Parallel Robots, 2nd Edition. Springer, Heidelberg, 2005
- [17] D. Chablat and P. Wenger, "Device for the movement and orientation of an object in space and use thereof in rapid machining", Centre National de la Recherche Scientifique /Ecole Centrale de Nantes, European patent: EP1597017, US patent: 20070062321, 2005
- [18] R. Clavel, "Delta, a fast robot with parallel geometry", Proc. 18th International Symposium on Industrial Robots, 1988, pp. 91-100
- [19] D. Chablat, and P. Wenger, "Architecture Optimization, of a 3-DOF Parallel Mechanism for Machining Applications, The Orthoglide," IEEE Trans. on Robotics and Automation, Vol. 19(3), 2003, pp.403-410
- [20] A. Pashkevich, P. Wenger and D.Chablat, "Design Strategies for the Geometric Synthesis of Orthoglide-type Mechanisms", Jr of Mechanism & Machine Theory, Vol. 40(8), 2005, pp. 907-930
- [21] A. Pashkevich, D.Chablat and P. Wenger, "Stiffness Analysis of 3-d.o.f. Overconstrained Translational Parallel Manipulators," Proc. IEEE Int. Conf. Rob. and Automation, May 2008
- [22] D. Chablat, and P. Wenger, "A six degree of freedom Haptic device based on the Orthoglide and a hybrid Agile Eye," 30th Mechanisms & Robotics Conference (MR), Philadelphia, USA, 2006.